Research Article Vol. 31, No. 20 / 25 Sep 2023 / Optics Express 31946

Optics EXPRESS

Peak-tracking BOTDA with dynamic ternary search

DI QI,[1] XUN GUAN,[2,3,*] YUANSEN CHENG,[1] AND CHUN-KIT CHAN[1]

[1] *Lightwave Communications Laboratory, Department of Information Engineering, The Chinese University of Hong Kong, Shatin, N.T., Hong Kong, China*
[2] *Tsinghua Shenzhen International Graduate School, Tsinghua University, Shenzhen, 518055, China*
[3] *Tsinghua-Berkeley Shenzhen Institute, Tsinghua University, Shenzhen, 518055, China*
[*] *xun.guan@sz.tsinghua.edu.cn*

Abstract: We propose a peak-tracking BOTDA (PT-BOTDA) equipped with an efficient dynamic Brillouin frequency shift (BFS) searching scheme based on ternary search. The proposed scheme establishes a feedback loop between the selected frequency and the corresponding Brillouin gain to reduce the required number of scanning frequencies in one measurement. We also demonstrate the performance evaluation of the proposed scheme under scenarios with different searching granularities and dynamic sensing ranges. Experimental results indicate that in all situations, the proposed PT-BOTDA can achieve at least 85% and 97% reduction in the number of scanning frequencies for 1-MHz and 0.1-MHz frequency steps, respectively, with a 3-meter spatial resolution, while maintaining a convincing BFS searching accuracy under sufficient SNR condition using a smaller searching interval.

1. Introduction

As one of the promising candidates of distributed optical fiber sensors, Brillouin optical time domain analyzer (BOTDA) has drawn significant research interest due to its remarkable capability of simultaneous temperature/strain monitoring [1] and long-haul distributed sensing [2]. The Brillouin frequency shift (BFS), typically extracted from the Brillouin gain spectrum (BGS) as the sensing target, changes linearly along the spectrum with the temperature/strain. However, the construction of the whole BGS in conventional frequency-sweeping BOTDA (FS-BOTDA) requires a frequency scanning process of hundreds of frequencies [3], which usually takes a couple of minutes. This time requirement makes FS-BOTDA hard to meet the distributed dynamic sensing requirements [4]. In [5], the author proposed a slope-assisted BOTDA which determined the BFS by measuring the Brillouin gain change of one single frequency on the slope of the BGS, thereby limiting the dynamic sensing range within the slope region. Although an engineered BGS extended the original sensing range by 70% in [6], it still did not adequately meet the requirement. In [7], the authors demonstrated a three-fold sensing range over the Brillouin linewidth, however coming with an increased measuring time when dealing with a larger BFS change. In [8] and [9], two single-shot BOTDA schemes were proposed to capture the whole BGS through one measurement by replacing the RF probe with an orthogonal frequency division multiplexing and optical chirp chain signal, respectively. Despite a faster measuring speed, these two implementations compromise in frequency or spatial resolution, limiting their performance compared to conventional FS-BOTDA [3]. In [10–12], compressed sensing was introduced to accelerate the frequency-sweeping process while at least 30% of the total frequencies were still needed for the BGS reconstruction in these schemes. In [13] and [14], BOTDA with a close-loop configuration was proposed and investigated, featured by continuously tracking and adjusting the Brillouin gain change of the target frequency using a proportional-integral-derivative controller. Nevertheless, the trade-off between convergence speed and BFS tracking accuracy

#500886 https://doi.org/10.1364/OE.500886
Journal © 2023 Received 20 Jul 2023; revised 31 Aug 2023; accepted 31 Aug 2023; published 11 Sep 2023

Optics EXPRESS

remains. Besides, although artificial neural network-based methods have demonstrated promising BFS estimation performance with a larger frequency-sweeping interval therefore revealing the potential of scanning frequency number reduction for conventional BOTDA [15–17], the network training requires a large amount of data and time.

In this paper, we report a novel peak-tracking BOTDA (PT-BOTDA) equipped with ternary search, an extremum-finding line-search algorithm for unimodal functions [18], to accelerate the BFS searching process dynamically. PT-BOTDA relies on a feedback loop, like [13] and [14]. However, the proposed method depends on the direct comparison result of the measured Brillouin gain rather than the computed slope, for a lower computational complexity. PT-BOTDA utilizes the conventional BOTDA setup, compromising no frequency/spatial resolution and being applicable to other proposed high-spatial-resolution schemes [19–21]. In addition, no Lorentzian curve fitting (LCF) operation is required. We have experimentally demonstrated that the proposed scheme can reduce the number of scanning frequencies over 85% and 97% for the 1-MHz and 0.1-MHz frequency step case, respectively, compared with the conventional full-span scanning.

2. Dynamic BFS ternary search

The theoretical Lorentzian model of the BGS naturally aligns with the ternary search algorithm [22]. The entire BGS is considered as a 1-D discrete unimodal array, whose dimension depends on the sensing range as well as the frequency granularity, with the BFS as the target peak. The distributed searching process operates by dynamically generating the probe frequency sequence. As depicted in Fig. 1, given the fiber length L and spatial resolution Δz, the entire sensing fiber can be divided into N consecutive sections, where $N = L/\Delta z$, corresponding to N consecutive frequency segments in the probe with the length of $2n_f\Delta z/c$, where c/n_f is the group velocity. For each section, the principle of dynamic searching is illustrated as follows:

1. Initialize f_{start}, f_{end}, where the dynamic range $D = f_{end}$ - f_{start}, and frequency granularity f_{step};
2. Calculate and scan the two trisection frequencies f_{left} and f_{right} with:
   - $f_{left} = f_{start} + round[D/(3 \times f_{step})] \times f_{step}$
   - $f_{right} = f_{end} - round[D/(3 \times f_{step})] \times f_{step}$
3. Calculate the average measured Brillouin gain G_{left}/G_{right} of f_{left}/f_{right} over the corresponding frequency segment length of $2n_f\Delta z/c$ and update the f_{start}/f_{end} with the following decisions:
   - If $G_{left} > G_{right}$, let $f_{end} = f_{right}$;
   - Else if $G_{left} < G_{right}$, let $f_{start} = f_{left}$;
   - Else if $G_{left} = G_{right}$, let $f_{start} = f_{left}$ and $f_{end} = f_{right}$.
4. Repeat 2-3 until $f_{left} = f_{right}$, then $BFS = f_{left}$.

Since the tracking process for each section is carried out in parallel, the distributed measuring time is approximately equivalent to that of a single section. The fact that $G_{left} = G_{right}$ in procedure 3) is rarely achieved, but this does not necessitate the introduction of a noise tolerance for its functionality. Consider a pair of measured G_{left} and G_{right} which are theoretically equal but practically unequal due to the presence of additive white Gaussian noise. The satisfaction of either condition $G_{left} < G_{right}$ or $G_{left} > G_{right}$ would not affect the convergence result. However, it would influence the convergence speed where only 1/3, instead of 2/3, of the current sensing range is eliminated. Besides, since at least 1/3 of the current tracking range will be always abandoned for each track, the tracking speed will be only determined by the required scanning

Optics EXPRESS

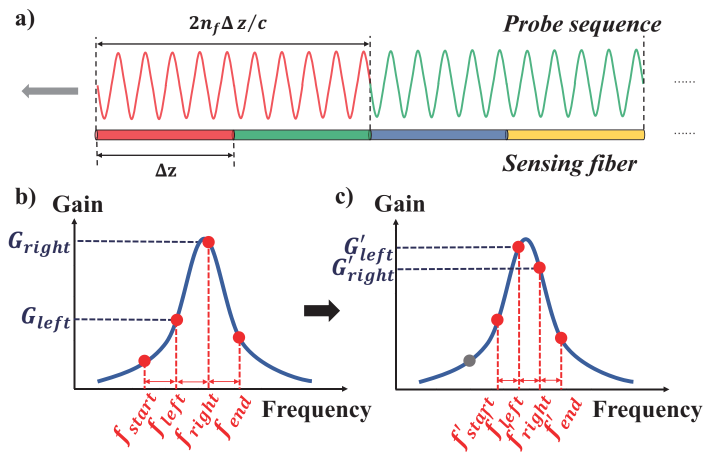

Fig. 1. Dynamic BFS ternary search on BGS. a) Schematic of the fiber segmentation and the corresponding probe frequency sequence; b) current searching and c) next searching on each section.

frequency number under the frequency-sweeping process. With two frequencies selected per measurement, the upper limit of the number of searched frequencies can be expressed as:

$$S(n) = S(\frac{2n}{3}) + 2 \approx 2\log_3 n \approx 4.19\,\lg n \tag{1}$$

where $n = R/f_{step}$ is the required number of scanning frequencies in FS-BOTDA and R is the total sensing range. Eq. (1) implies higher reduction efficiency with an increasing n. This property can also be illustrated that for a fixed sensing range R, the BFS searching efficiency can be enhanced by a smaller f_{step}. Furthermore, it should be noted that the frequency resolution of the proposed method is directly limited by the frequency granularity. In this case, a smaller f_{step} can also serve as a good compensation.

3. Numerical simulation

We conducted the frequency reduction efficiency test with 13 groups of different scanning range L: 10, 50, 100, 150, 200, 250, 300, 350, 400, 450, 500, 550, and 600 MHz. The frequency granularity was 1 MHz so $n = L$. The BFS was set at 10.890 GHz and was maintained at the center of the scanning range for each testing group. For example, the 600-MHz scanning range spanned from 10.590 GHz to 11.189 GHz, and from 10.885 GHz to 10.894 GHz for the 10-MHz group. The Brillouin linewidth was set at 35 MHz, compatible with the BGS generated by the pump pulse width used in the experiment. The signal-to-noise ratio (SNR) was set to 20 dB, and the average scanned frequency number (ASFN) was calculated from 500 repeated measurements. Figure 2 shows the simulation result with the proposed peak-tracking (PT) scheme, benchmarked by the conventional BOTDA case where the frequency-sweeping (FS) process was adopted. The ASFN of the proposed scheme exhibited a logarithmic relationship with increasing n, fitting the curve of $4.2\lg n$. This agreed with Eq. (1), while FS-BOTDA presented a linear one. The black dashed line indicated that the ratio of the scanned frequency of the proposed scheme over that of the FS scheme decreased inverse-proportionally with n as mentioned above, exceeding 96% when the sensing range reached 600 MHz.

To verify the consistency of the tracing speed over the whole sensing range, we have simulated another four test sets with the sensing range of 120, 300, 600, and 1200 MHz correspondingly, all of which centered at 10.89 GHz with a frequency regularity of 1 MHz. The Brillouin linewidth

Optics EXPRESS

was all set to 35 MHz. Each set contained five uniformly distributed tracing targets. For example, in the 120-MHz sensing range, the BFS targets were 10.85, 10.87, 10.89, 10.91, and 10.93 GHz, while in the 1200-MHz set, they were 10.49, 10.69, 10.89, 11.09, and 11.29 GHz. Figure 3 shows the ASFN for every target BFS with 500 measurements, where the BFS portion is calculated by

$$BFS\ portion\ (\%) = \frac{BFS - f_{start}}{f_{end} - f_{start}} \tag{2}$$

where f_{start}/f_{end} is the start/end frequency for each set. As the total sensing range increased, the ASFN presented a "W-shaped" tendency along the spectrum where smaller ASFNs were located at the trisection points of the whole range owing to the nature of ternary search. Nevertheless, the maximum ASFN difference was less than 1.5, indicating a consistent tracing speed over the diverse range of BFS.

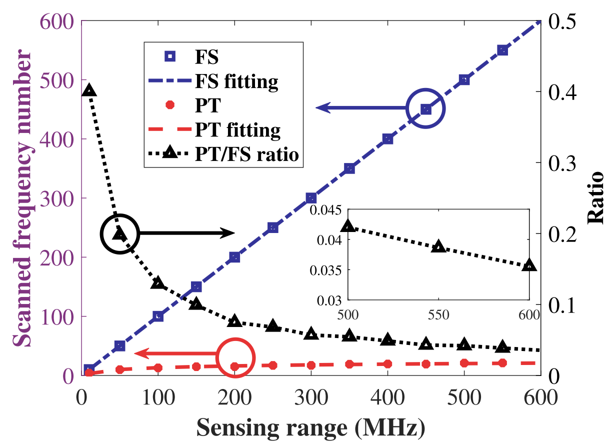

Fig. 2. Simulation of the proposed PT scheme and the conventional FS scheme on the number of scanned frequencies. The blue and red curves are on the left axis while the black curve is on the right axis. The inlet is the partial enlargement where the sensing range L gets larger than 500 MHz.

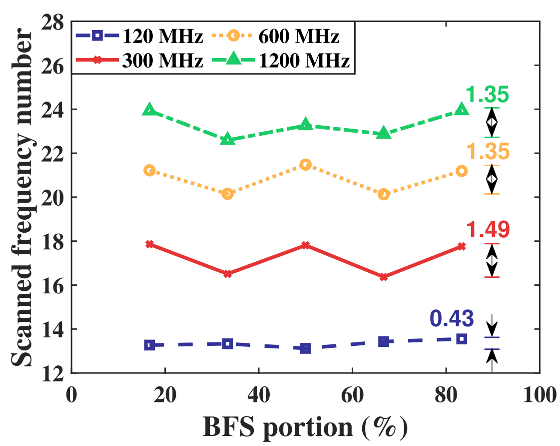

Fig. 3. Simulation of ASFN of the proposed PT scheme on different BFS locations with respect to different sensing ranges.

4. Experiment and discussion

Figure 4 shows the experimental setup. The light source was a 100-kHz-linewidth tunable laser, operating at 1549.6 nm. The output beam was divided by a 50/50 coupler into two branches. The probe (the upper branch) was modulated by an intensity modulator operating in the carrier-suppression mode, driven by an electrical signal that mixed a continuous wave as the frequency offset generated by an analog signal generator and a frequency-agile sequence as the dynamic searching probe. The frequency-agile sequence was generated by an arbitrary waveform generator (AWG) running at a sampling rate of 5 GS/s, to provide enough bandwidth. The frequency offset and the searching sequence frequency could be adjusted according to the sensing range and the frequency step. In practice, the generation of this probe frequency sequence could be realized using a voltage-controlled oscillator for simplicity, which would significantly reduce the receiver sampling rate. The pump (the lower branch) was firstly modulated by a high extinction-ratio modulator (>30 dB) to generate a 30-ns pump pulse, whose peak power was amplified to 20 dBm before being launched into the fiber under test (FUT). With the head 3-meter section heated by a water bath, the FUT was a 60-meter polarization-maintaining fiber for polarization noise compression. The polarization noise could be dynamically addressed by polarization multiplexing in the pump [23] if a single-mode fiber was adopted. Two polarization beam splitters were deployed on both sides of the FUT to align the states of polarization with two polarization controllers, and an optical isolator was placed on the probe side to block the reflection and the counter-propagating high-power pump signal. After the band-pass filter and pre-amplification, the Stokes part of the probe was selected and fed into a 40-GHz photodetector, followed by a 210-MHz electronic filter. Finally, the Brillouin signal was collected by a digital storage oscilloscope with a sampling rate of 20 GS/s before being processed in MATLAB. As previously mentioned, the data samples within one probe frequency segment would be averaged for the Brillouin gain calculation where a high sampling rate might enhance the SNR. However, this would not affect the validation of our scheme, since the same operation was conducted for the conventional setup.

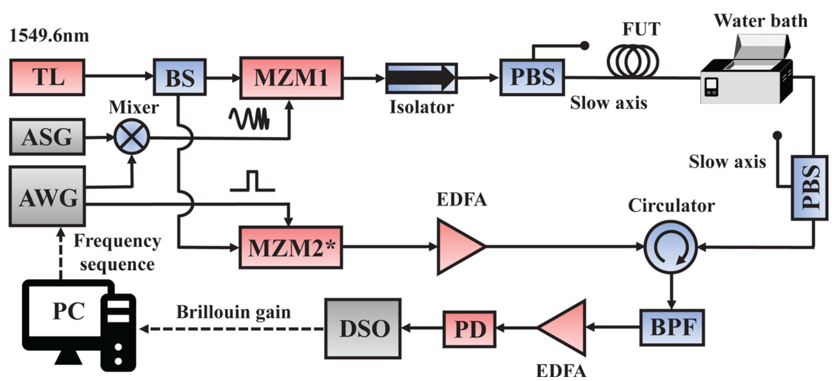

Fig. 4. Experimental setup. TL: tunable laser, AWG: arbitrary waveform generator, ASG: analog signal generator, BS: beam splitter, MZM: Mach-Zehnder modulator (*: high extinction ratio), EDFA: Erbium-doped fiber amplifier, PBS: polarization beam splitter, FUT: fiber under test, BPF: bandpass filter, PD: photodetector, DSO: digital storage oscilloscope, PC: personal computer. The polarization controllers used before modulators and the BPFs after EDFAs are omitted.

We first validated the temperature sensing capability of the proposed scheme. Figure 5 shows the searching results under different temperatures. The temperature was set from 30° to 50° with an increment of 5°, and the frequency resolution was 1 MHz. The triangles represented the BFS searching results by PT, while the squares were obtained by LCF. A good consistency in the BFS-temperature fitting curves was observed between the proposed PT-BOTDA and the conventional one. The linear fitting coefficient of the proposed scheme was 0.9971 with a temperature sensitivity of 1 MHz/°. The temperature tracking accuracy can be further improved by using a smaller tracing step, which will be discussed later.

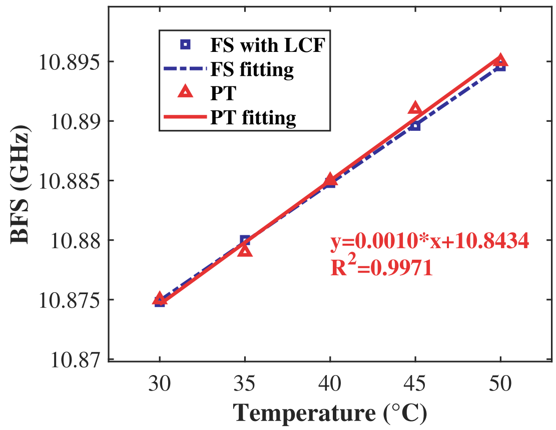

Fig. 5. BFS-temperature curve of both conventional FS-BOTDA using LCF (blue) and proposed PT-BOTDA (red).

Next, we conducted simulations and experiments to explore the influence of varying sensing ranges on the BFS search accuracy. Figure 6 shows the search performance of the proposed scheme at a temperature of 40°, with sensing ranges of 60, 100, 300, and 600 MHz centered at 10.890 GHz, and a frequency step of 1 MHz. The simulated 35-MHz Brillouin linewidth closely matched the measured result. The root mean square error (RMSE) was calculated based on 50 measurements, each with 50-time averaging to ensure a 20-dB SNR condition. The discrepancy of RMSE between the measurement and simulation was due to the non-unimodal spectral response. Both solid curves showed that an increasing sensing range led to a decreasing RMSE, providing strong evidence that the proposed scheme did not compromise tracing speed and accuracy. This observation could be explained as follows: for a BGS with a certain Brillouin linewidth, a larger sensing range reduces the likelihood of searching trials falling within the BGS region, thereby minimizing searching errors induced by additive white Gaussian noise. The dash lines below presented the scanned frequency number ratio of our scheme over FS-BOTDA. When the sensing range increased to 600 MHz, the measured PT/FS ratio was only 0.0383, which perfectly matched the result in Fig. 2.

We also investigated the search accuracy with different frequency steps. Figure 7 illustrates the BFS searching accuracy comparison between PT-BOTDA and FS-BOTDA with 1-MHz and 0.1-MHz frequency steps under different noise levels. It should be noted that the 0.1-MHz step size was selected as the representative of a smaller sweeping step for the demonstration purpose without practical reference. When the SNR was relatively insufficient, it appeared that a smaller frequency step size did not benefit the search accuracy as predicted. In fact, the 1-MHz case even outperformed the 0.1-MHz case when the temperature exceeded 40°. This observation could be attributed to more search trials falling into the BGS region with a smaller frequency step. In such a case, the insufficient SNR caused a higher search error probability for each trial and eventually the result. This explains the phenomenon that the 0.1-MHz case outperformed the 1-MHz case with higher SNR, reducing the overall RMSE to 0.45 MHz. On the other hand, under similar noise levels, the proposed method exhibited worse search accuracy compared to the conventional LCF method due to the intrinsic frequency resolution limitation. However, this was accomplished with less than 15% and 3% (for the 1-MHz and 0.1-MHz step, respectively)

Optics EXPRESS

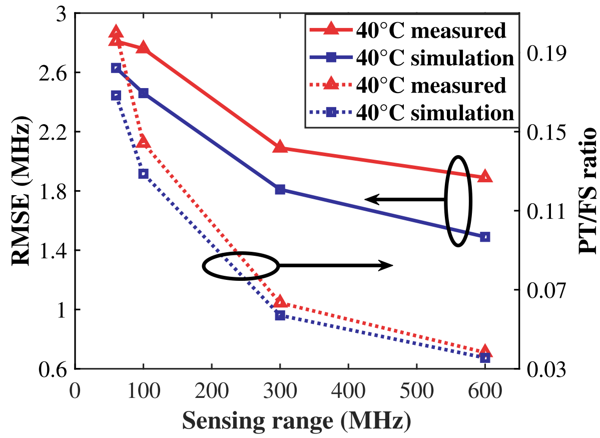

Fig. 6. RMSE of searched BFS under 40° and the scanned frequency ratio over conventional setup with different sensing ranges. The solid curves are on the left axis while the dash curves are on the right axis.

of the scanned frequency number. In addition, with 500-time averaging, the mean temperature searching uncertainty of the proposed method was only 0.15° larger than that of the conventional LCF method for the 0.1-MHz case. This verified that, with a smaller frequency step, the proposed PT-BOTDA could achieve competitive BFS searching accuracy to FS-BOTDA under sufficient SNR conditions. able 1 presents the ASFN of 50 measurements under different temperatures with 1-MHz and 0.1-MHz frequency steps. Given the whole sensing range was 100 MHz, it could be found that even the average count slightly differed among temperatures, the reduction efficiency was at least 85% for 1-MHz cases and 97% for 0.1-MHz cases compared with the FS-BOTDA.

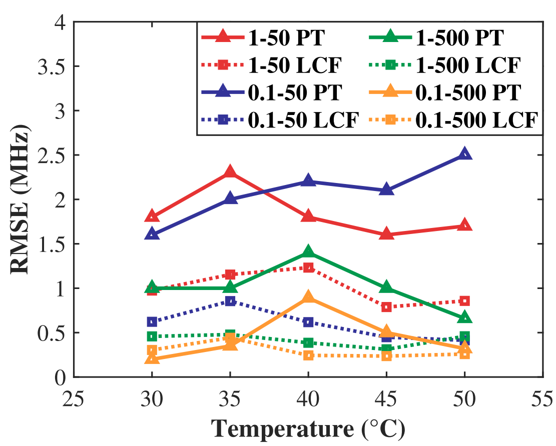

Fig. 7. RMSE of searched BFS comparison between the proposed PT method and the conventional LCF under different temperatures with different frequency step size and averaging times, where "1-50" means 1-MHz step with 50-time averaging.

Finally, we carried out the distributed sensing experiment. Figure 8 shows the distributed BFS measured along the 60-meter FUT at different heating temperatures with a frequency resolution of 1 MHz. For the first 3-meter heating part under different heating temperatures of 30°, 40° and 50°, the corresponding BFS search results were 10.876 GHz, 10.885 GHz, and 10.894 GHz, showing a great agreement with the theoretical values derived in Fig. 5. For the unheated part,

Optics EXPRESS

Table 1. Measured Average scanned frequency number under various temperatures

Temperature (°)	1-MHz Step		0.1-MHz Step	
	Frequency Count	Reduction Ratio	Frequency Count	Reduction Ratio
30	12.64	87.36%	24.28	97.57%
35	14.10	85.90%	24.48	97.55%
40	14.42	85.58%	24.14	97.59%
45	13.24	86.76%	24.40	97.56%
50	13.74	86.26%	24.66	97.53%

the BFS discontinuity for three measurements was due to the tracking error which was at least equal to the frequency resolution. The maximum BFS searching disagreement was found to be 4 MHz in the near-heating section. This discrepancy might be due to the ghost peak generated by the sharp frequency change within the BGS region in the continuous frequency chain [9]. This issue could be addressed by conducting the second measurement with a pump-probe delay shift, as in [24]. With a 100-MHz sensing range and a 1-MHz step, PT-BOTDA only took 6.1 seconds for one distributed measurement (mainly limited by the AWG data upload speed), showing a 33.1-fold acceleration compared to the 201.9 seconds required for FS-BOTDA. Specially, this acceleration could be further improved with an extension of the sensing distance, due to the parallel BFS peak-tracking nature of PT-BOTDA, which significantly saves time compared to the distributed LCF operation.

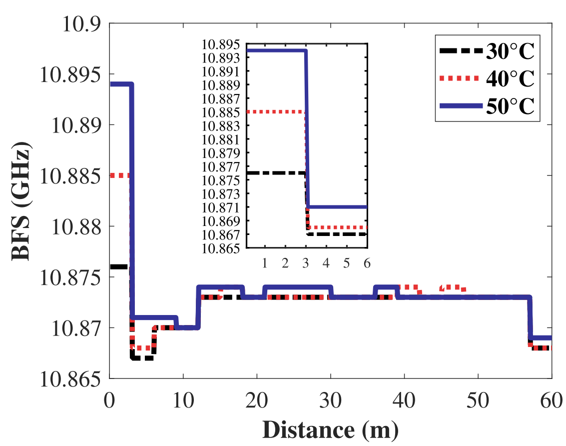

Fig. 8. Distributed BFS under different temperatures along the FUT. The inlet is the partial enlargement at the heating part.

5. Conclusion

In this paper, we have proposed a PT-BOTDA scheme to efficiently reduce the scanned frequency number in BOTDA frequency retrieval. The proposed method offers low computational complexity and achieves an unlimited sensing range without any trade-off between tracking speed and accuracy, where it outperforms the close-loop BOTDA in [13,14] and the slope-assisted BOTDA in [5]. Experimental results have demonstrated that our scheme can reduce the required scanned frequency number by more than 85% and achieve a measuring time that is only 3%

Optics EXPRESS

of that of conventional BOTDA while maintaining comparable BFS searching accuracy under sufficient SNR. These results highlight the significant application potential of the proposed PT-BOTDA in scenarios with large sensing ranges.

Funding. National Key Research and Development Program of China (2021YFA1001000); Science, Technology and Innovation Commission of Shenzhen Municipality (JCYJ20220530142809022, WDZC20220811170401001).

Disclosures. The authors declare no conflicts of interest.

Data availability. Data underlying the results presented in this paper are not publicly available at this time but may be obtained from the authors upon reasonable request.

References

1. A. Motil, A. Bergman, and M. Tur, "Temperature and strain discrimination in BOTDA fiber sensor by utilizing dispersion compensating fiber," IEEE Sens. J. **18**(17), 7100–7105 (2018).
2. Y. Dong, B. Wang, C. Pang, D. Zhou, D. Ba, H. Zhang, and X. Bao, "150km fast BOTDA based on the optical chirp chain probe wave and Brillouin loss scheme," Opt. Lett. **43**(19), 4679–4682 (2018).
3. T. Horiguchi, K. Shimizu, T. Kurashima, M. Tateda, and Y. Koyamada, "Development of a distributed sensing technique using Brillouin scattering," J. Lightwave Technol. **13**(7), 1296–1302 (1995).
4. K. Hotate and S. S. L. Ong, "Distributed dynamic strain measurement using a correlation-based Brillouin sensing system," IEEE Photonics Technol. Lett. **15**(2), 272–274 (2003).
5. Y. Peled, A. Motil, L. Yaron, and M. Tur, "Slope-assisted fast distributed sensing in optical fibers with arbitrary Brillouin profile," Opt. Express **19**(21), 19845–19854 (2011).
6. C. Feng, H. D. Bhatta, J. Bohbot, R. Davidi, X. Lu, T. Schneider, and M. Tur, "Gain spectrum engineering in slope-assisted dynamic Brillouin optical time-domain analysis," J. Lightwave Technol. **38**(24), 6967–6975 (2020).
7. D. Ba, B. Wang, D. Zhou, M. Yin, Y. Dong, H. Li, Z. Lu, and Z. Fan, "Distributed measurement of dynamic strain based on multi-slope assisted fast BOTDA," Opt. Express **24**(9), 9781–9793 (2016).
8. J. Fang, P. Xu, Y. Dong, and W. Shieh, "Single-shot distributed Brillouin optical time domain analyzer," Opt. Express **25**(13), 15188–15198 (2017).
9. D. Zhou, Y. Dong, B. Wang, C. Pang, D. Ba, H. Zhang, Z. Lu, H. Li, and X. Bao, "Single-shot BOTDA based on an optical chirp chain probe wave for distributed ultrafast measurement," Light: Sci. Appl. **7**(1), 32 (2018).
10. D. Zhou, W. Peng, L. Chen, and X. Bao, "Brillouin optical time-domain analysis via compressed sensing," Opt. Lett. **43**(22), 5496–5499 (2018).
11. Q. Chu, B. Wang, H. Wang, D. Ba, and Y. Dong, "Fast Brillouin optical time-domain analysis using frequency-agile and compressed sensing," Opt. Lett. **45**(15), 4365–4368 (2020).
12. H. Zheng, Y. Yan, Z. Zhao, T. Zhu, J. Zhang, N. Guo, and C. Lu, "Accelerated fast BOTDA assisted by compressed sensing and image denoising," IEEE Sens. J. **21**(22), 25723–25729 (2021).
13. Z. Yang, M. A. Soto, D. M. Chow, P. Ray, and L. Thévenaz, "Brillouin distributed optical fiber sensor based on a closed-loop configuration," J. Lightwave Technol. **36**(5), 1239–1248 (2018).
14. L. Zhang, A. G. Correa-Mena, Z. Yang, F. Sauser, S. L. Floch, and L. Thévenaz, "Closed-loop technique based on gain balancing for real-time Brillouin optical time-domain analysis," Opt. Lett. **47**(17), 4299–4302 (2022).
15. A. K. Azad, L. Wang, N. Guo, H.-Y. Tam, and C. Lu, "Temperature sensing in BOTDA system by using artificial neural network," Electron. Lett. **51**, 1578–1580 (2015).
16. A. K. Azad, L. Wang, N. Guo, H.-Y. Tam, and C. Lu, "Signal processing using artificial neural network for BOTDA sensor system," Opt. Express **24**(6), 6769–6782 (2016).
17. Z. Cao, N. Guo, M. Li, K. Yu, and K. Gao, "Back propagation neutral network based signal acquisition for Brillouin distributed optical fiber sensors," Opt. Express **27**(4), 4549–4561 (2019).
18. W. Anggoro, in *C++ Data Structures and Algorithms*, (Packt Publishing, 2018).
19. A. W. Brown, B. G. Colpitts, and K. Brown, "Distributed sensor based on dark-pulse Brillouin scattering," IEEE Photonics Technol. Lett. **17**(7), 1501–1503 (2005).
20. K. Kishida, C.-H. Li, and K. Nishiguchi, "Pulse prepump method for cm-order spatial resolution of BOTDA," Proc. SPIE **5855**, 559 (2005).
21. W. Li, X. Bao, Y. Li, and L. Chen, "Differential pulse-width pair BOTDA for high spatial resolution sensing," Opt. Express **16**(26), 21616–21625 (2008).
22. A. Yeniay, J.-M. Delavaux, and J. Toulouse, "Spontaneous and stimulated Brillouin scattering gain spectra in optical fibers," J. Lightwave Technol. **20**(8), 1425–1432 (2002).
23. D. Qi, J. Li, X. Guan, and C. K. Chan, "Dynamic polarization-insensitive BOTDA in direct-detection OFDM with CNN-based BFS extraction," Opt. Express **30**(5), 7725–7736 (2022).
24. S. Wang, Z. Yang, S. Zaslawski, and L. Thévenaz, "Short spatial resolution retrieval from a long pulse Brillouin optical time-domain analysis trace," Opt. Lett. **45**(15), 4152–4155 (2020).